Available online at www.sciencedirect.com
SCIENCE DIRECT
International Journal of Multiphase Flow 32 (2006) 623–642
International Journal of Multiphase Flow
www.elsevier.com/locate/ijmulflow

Shock tube study of the dynamical behavior of granular materials

A. Britan, G. Ben-Dor *

Pearlstone Center for Aeronautical Engineering Studies, Department of Mechanical Engineering, Ben-Gurion University of the Negev, Beer-Sheva, Israel

Received 30 March 2005; received in revised form 19 January 2006

Abstract

The purpose of the present study is to clarify both the compression phenomenon and the gas filtration effect that take place inside a granular medium when it is dynamically loaded by a shock wave. In order to measure the pore pressure and the total stress at different locations along the granular medium, pressure transducers were placed along the side-wall and at the end-wall of the shock tube test section, which was filled with the granular material. In order to elucidate the gas filtration effect, the results of two experiments with identical granular media but with and without filtration were compared. The gas filtration was eliminated by means of a thin plastic film, which was placed at the front edge of the granular medium. Based on this comparison quantitative information on the gas filtration and its role in the stress formation inside granular media of different material and length was obtained. Furthermore, curves of the dynamic compression and the Young moduli of the granular medium for the range of the operating conditions were reconstructed.

Keywords: Granular materials; Cellular materials; Compaction waves; Filtration; Pressure loading

1. Introduction

The dynamical behavior of granular media subjected to unsteady pressure loadings is one of the most interesting subjects of research in the mechanics of multiphase flows (see e.g., Nesterenko, 2001; Holster and Brennen, 2005a; Sen et al., 2005). While the mathematical models of the main processes that are involved are known, the phenomenon is not fully understood yet and the governing equations can be solved in terms of measurable macroscopic parameters only for some discrete conditions (Bear and Bachmat, 1990; Holster and Brennen, 2005b). Hence, most of the information available on the features of granular media is based on experimental studies.

From a broad spectrum of the experimental data it is evident that the response of a granular medium to compression depends on the loading conditions. Specifically it was shown (see e.g., Blazynsky, 1987), that

* Corresponding author. Fax: +972 8 6472969.
E-mail address: bendorg@bgumail.bgu.ac.il (G. Ben-Dor).

0301-9322/$ - see front matter © 2006 Elsevier Ltd. All rights reserved.
doi:10.1016/j.ijmultiphaseflow.2006.01.007

while static and dynamic loadings resulted in similar post-loading densities of the granular compound, the strength of a compound which was dynamically consolidated increased 1.5–2.5 times more than one which was loaded statically. It is well established now, that the gaseous phase processes inside the granular medium and the rate effects of the loading are the major contributing factors to the difference. While in static laboratory tests, the gas filling the pores between the granules can be freely pushed out, in a short time impact, the granular medium behaves as a closed system of constant content. The unsteady waves of the shock induced filtration, interact with the rigid skeleton as well as with the air entrapped between the particles and affect the dynamics of the pore compression (see e.g., Baer, 1988; Britan et al., 1995).

A typical example of such a complex two-phase system, which has been extensively studied since the early 1970s, is a shock wave impact on the layer of permeable foam (Gelfand et al., 1975; Gvozdeva et al., 1985). Experimental observations of Skews et al. (1993) and van Dongen et al. (1995) provided probably the first evidences that the gas flows both into and out of the foam.

This, in turn, resulted in separate waves in the gas and in the foam skeleton. This improved an earlier conclusion of Skews (1991) and Gvozdeva et al. (1993) that the common assumption of a simple pseudo-gas theory that the foam interface is a gas contact surface was not correct. Much effort has been spent to explain why a foam protected pressure transducer shows pressure amplification as compared to that without foam (Gelfand et al., 1983; Bazhenova et al., 1986; Raevsky et al., 1990; Ben-Dor et al., 1994). Recent results of Yasuhara et al. (1996), Gvozdeva et al. (1996), Seitz and Skews (1996) and Igra et al. (1997) have provided fresh insight into this problem.

Based on past findings it was shown that the shock induced filtration of the gas inside the foam resulted in a front of collapsed foam cells which, in turn, resulted in an extremely large resistance to the gas flow. Skews et al. (1993) referred to this front as a ''piston'' which pushed the gas towards the low-pressure open pores of the non-collapsed foam. The gas flow ahead of the piston was finally brought to rest owing to the pressure rise in the ever-reducing volume ahead of it and the fact that the gas was captured near the end-wall was discussed in detail by Seitz and Skews (1996). Different conditions govern the gas filtration and the stress formation on either side of this piston. Behind the piston the foam stiffness and its capability to recover (Gvozdeva et al., 1996) influence the gas flow. The stress ahead of the piston depends on the drag characteristics of the uncompressed cells and on the conditions at the piston front. The results of the recent shock tube experiments of Yasuhara et al. (1995, 1996) that are reproduced in Figs. 1 and 2 offer a fertile field to illustrate the role of the piston effect and other components on the stress formation. All these data were obtained with foams or a rubber and an incident shock wave Mach number $M_s = 1.7$. As in similar cases the pressure transducer for the gas pressure measurement was not in contact with the sample skeleton and the stress was related to the total stress σ_t, or the sum of the stress and the gas pressure P. In the following these results are considered in more details.

Since the gas flow inside the rubber is fully eliminated, the highest peak $\sigma_t = \sigma_{t\max}$ in the signal shown in Fig. 1a is the maximum stress experienced by the rubber in the uni-axial stress loading without filtration effects. The peak stress for this case is followed by dumping vibrations which eventually approach the steady pressure obtained behind the reflected wave, P_5, and the pressure amplification factor is $\delta_m = (\sigma_{t\max}/P_5) = 2.6$. Additional results in the figures refer to polyurethane foams having porosities $\pi = 0.76$ and $\pi = 0.98$. Specifically, the signals in Fig. 1b were obtained with a foam composed of small cells (named as foam slab F1 in this figure). It is clear that gas filtration inside the foam results in very slow increase of the pressure P, while, the variation in σ_t appears as a sharp narrow spike with an amplification factor of $\delta_m = 3.3$. Note that the spike duration (Fig. 1b) is nearly twice shorter than that in the rubber (Fig. 1a). Although a foam with a small pore structure and a light-mobile skeleton (its density is more than four times smaller than that of the rubber) is more productive in formation of the peak stress than rubber, the gas flow through these foams is retarded strongly and its mobility is negligibly small.

The density of foams F2 and F3 in Fig. 2 is more than 10 times smaller than that of F1. They can be readily compressed and hence, stronger and narrower peak stresses for these foams were expected. The signals in Fig. 2 clearly show that this is not the case. In contrast to the data in Fig. 1b the total stress profile, σ_t, correlate well with the gas pressure, P. The reason for such a correlation, which by itself is a clear evidence of the piston effect inside the porous medium (see Britan et al., 1997b), lies in the fact that these foams consist of larger cells and they have larger porosities. The strong transmitted wave compressing the slab reaches the

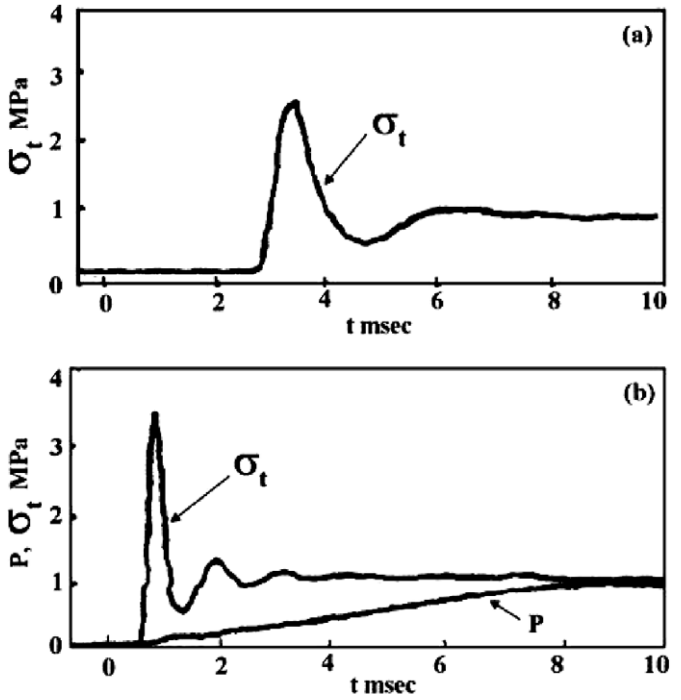

Fig. 1. (a) Total stress history, σ_t, at the shock tube end-wall covered with the rubber (Yasuhara et al., 1995). Slab length $h = 30$ mm, porosity $\pi = 0$ and density $\rho_c = 1.219$ g/cm^3. (b) Gas pressure, P, and total stress, σ_t, at the shock tube end-wall covered by foam F1 (Yasuhara et al., 1996). Slab length $h = 30$ mm, porosity $\pi = 0.76$ and density $\rho_c = 0.28$ g/cm^2.

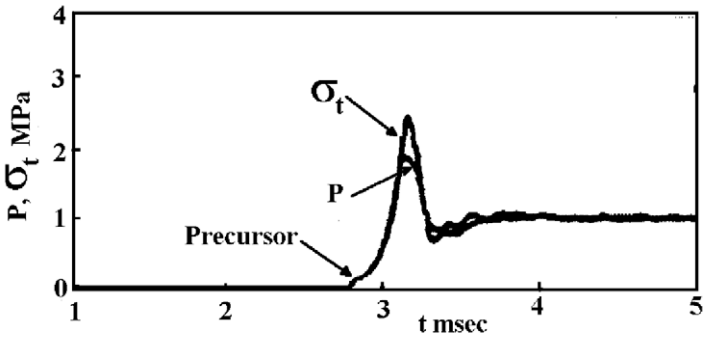

Fig. 2a. Gas pressure, P, and total stress, σ_t, at the shock tube end-wall covered by foam F2 (Yasuhara et al., 1996). Slabs length $h = 60$ mm, porosity $\pi = 0.98$ and bulk density $\rho_c = 0.026$ g/cm^3.

end-wall ahead of the piston and the gas accumulated near the end-wall acts like a buffer reducing the pressure amplification factor from about $\delta_m = 1.7$ for F2 to about $\delta_m = 1.1$–1.2 for F3. From comparing the data in Figs. 1 and 2, one can conclude that the gas filtration ahead of the piston is negligibly small inside the rubber and the low porosity foam F1, while it clearly manifests itself as a precursor in the stress signals obtained with the foam samples F2 and F3. The amplitude of the precursor (and hence, the role of the filtration) increases with the foam porosity and cell size. Therefore, the precursor comprises about half of the stress signal for the foam sample F3. In other words, when the drag characteristics of the skeleton decrease (larger cells size) most of the total stress, σ_t, is attributed to the gas filtration.

Fig. 3, which reproduces the results obtained by Gvozdeva et al. (1985) and by Ben-Dor et al. (1994), shows that at least two mechanisms are involved in the stress formation. One involves the stress peak that is seen to

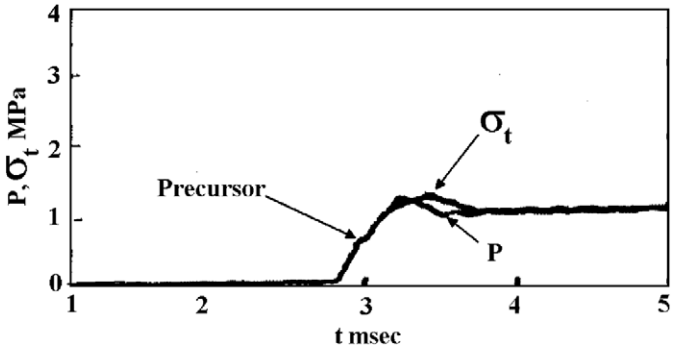

Fig. 2b. Total stress, σ_t, and gas pressure, P, at the shock tube end-wall (Yasuhara et al., 1996) covered by foam F3, $h = 60$ mm.

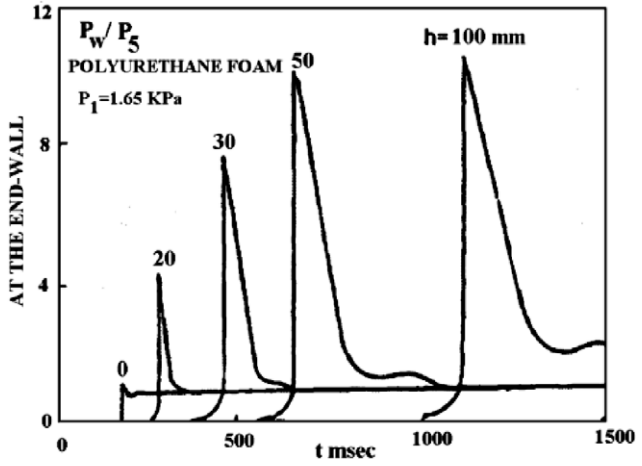

Fig. 3a. The pressure histories at the shock tube end-wall for polyurethane foams with different initial lengths and $M_s = 5$ (Gvozdeva et al., 1985).

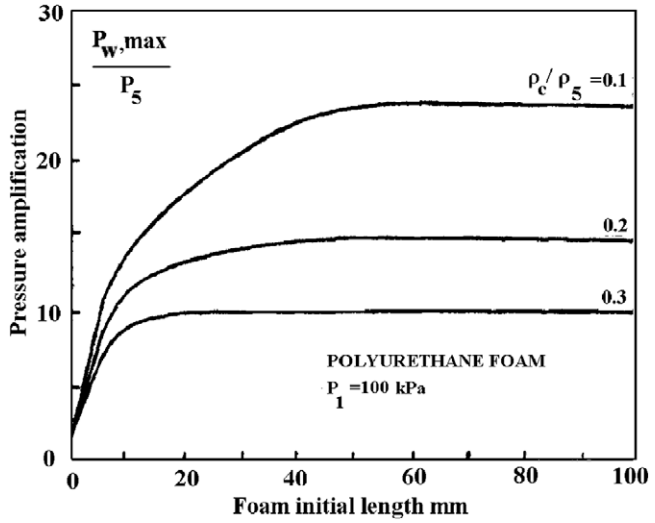

Fig. 3b. The dependence of the calculated peak pressure at the shock tube end-wall on the initial length of the foam and its relative density (Ben-Dor et al., 1994).

increase with the slab length, h, because of the increase in the mass of the foam skeleton, which is stagnated at the end-wall. The other, is associated with the increase in the stress that is experienced by the foam skeleton due to the filtration drag force, which depends of the foam density. While, the net resistance of the cells to the gas filtration also increases with h, once an "optimal" length h^* of the foam layer is reached, the majority of the gas remains compressed within the skeleton and it does not participate in the formation of the gas pressure peak at the end-wall (Seitz and Skews, 1996). While the peak pressure in Fig. 3a for samples of lengths $h = 50$ and $h = 100$ mm are similar, in Fig. 3b the optimal length h^* for samples of different densities is changed from $h^* < 20$ mm for $\rho_c/\rho_0 = 0.3$ to $h^* > 60$ mm for $\rho_c/\rho_0 = 0.1$.

In summary, one can say that when the shock tube end-wall is protected by a layer of a flexible foam, the cell size, the foam porosity, its density and the sample length are the most important parameters dominating the profile and peak of the registered total stress.

2. Aim of the present study

Bearing in mind the foregoing introduction, the key questions to be addressed in the present study are:

(i) What happens with the stress characteristics if the flexible foam that covers the shock tube end-wall is replaced by a layer of rigid granules whose stiffness and resistance to the gas filtration are well above that of the foam?
(ii) How does the gas filtration contribute to the stress formation during the impact of a weak shock wave on the granular column?
(iii) How can one use the total stress and the gas pressure signals to understand the unsteady flow pattern inside the granular medium?
(iv) Is it possible to use total stress measurements to reconstruct the compressive curves for the dynamic impact on the granular materials inside the shock tube?

3. Experimental set-up

The experiments were conducted in a vertical shock tube, which was described previously by Ben-Dor et al. (1997). The shock tube (see Fig. 4) was made of a steel tube of a square 31 mm × 31 mm cross-section. The Mach number of the incident shock wave was about $M_s = 1.3$ and did not vary significantly between the experiments. The test sections of different lengths were instrumented by pressure transducers T1, T3, T5, T7 which were isolated from a direct contact with the granular particles by a screen permeable to the gas. This was done in order to measure the local gas pressure inside the layer. Pressure transducers T2, T4, T6 and T8 were installed without an isolating screen in order to measure the compressive stress. The recorded data were stored using a data acquisition system GageScope sampling at 500 kHz per channel on an IBM-486 computer.

All the experiments were conducted with test sections of four different lengths: $h = 138$ mm, $h = 94$ mm, $h = 64$ mm and $h = 44$ mm. The length of each test section was identical to that of the tested granular sample. Prior to each experiment the test section was lifted of the holding flange in order to fill it to its full depth with the investigated granular material. In order to improve repeatability of the initial conditions and homogeneity of the granular layer, light knocking was applied on the test section walls during the filling process. Once the preparation procedure was completed the test section was bolted back to the rear flange of the low-pressure chamber.

The properties of the granular materials that were used in the present study are given in Table 1. The mean diameter of the granules, d_p, for material N2 was measured by a microscope with an accuracy of ±0.01 mm. Powders N1 and N3 were grated using sieves with calibrated mesh sizes. The bulk densities, ρ_c, were determined from the overall layer volume and its weight in air. The initial porosity of the granular layer was calculated from: $\pi = 1 - \rho_c/\rho_p$ and for the permeability of the granular layer, f, the well-known Carman–Cozeny formula, derived for an isotropic bulk of mono-spherical particles, was used (for more details see e.g., Dullien, 1992). Hereafter, the code number assigned in Table 1 will identify each tested material in the text and figures.

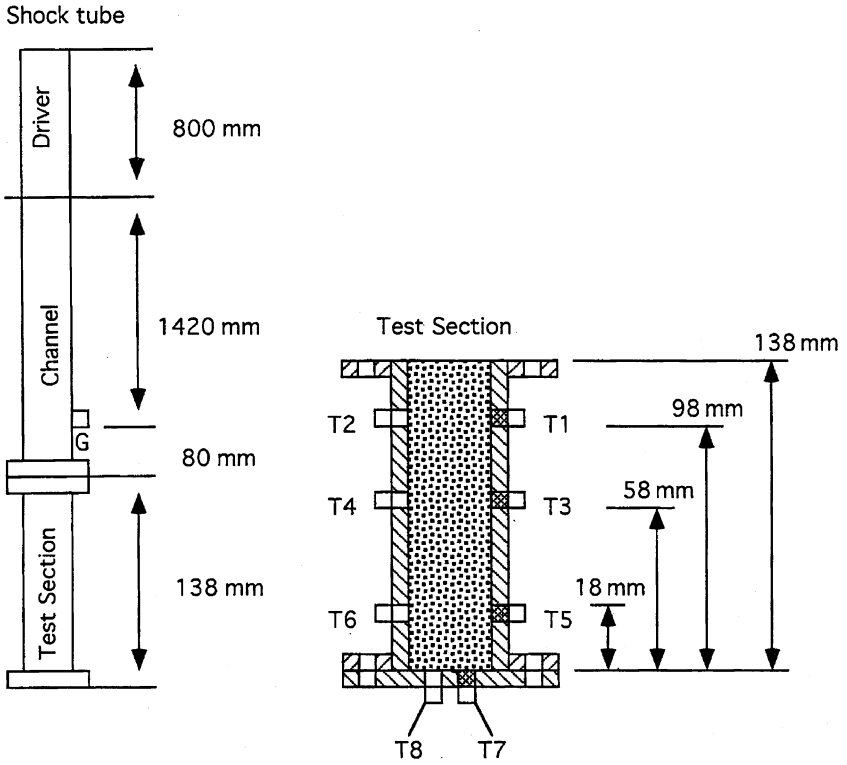

Fig. 4. Schematic illustration of the shock tube and the test section that were used in the experimental study (all the dimensions are in mm).

Table 1
Properties of the granular materials which were used in the experiments

N	Material	d_p, mm	ρ_c, g/cm^3	π	f, mm^2
1	Potash	0.45	1.089	0.428	0.00027
2	Fe	1.04	4.499	0.393	0.00099
3	Fe	0.45	4.457	0.399	0.00018

d_p – diameter, ρ_c – bulk density, π – initial porosity, f – permeability.

4. Experimental results

4.1. Shock wave homogenization and role of filtration in the stress formation

When a weak shock wave impacts on the porous material, the total stress measurements inside the sample may depend on the material characteristics. From gasdynamic point of view the main difference between a foam layer and a bulk of granules is the difference in the skeleton structure.

During the foam compression it undergoes extremely large deformations (Skews et al., 1993), and hence, the speed of the wave and its interaction at the sample boundaries largely govern the amplitude and the profile of the total stress. Consequently, when the foam porosity increases a stronger transmitted wave compresses the foam and after its reflection at the end-wall, it interacts with the foam interface. As a result the time duration and amplitude of the total stress peak are reduced. These characteristics of the total stress decrease when the foam porosity increases are demonstrated quite well in Figs. 1–3.

Notably, the granular medium porosity is much smaller and its compression during the impact by a weak shock wave is negligible. Thus, the boundary interactions affect the stress profile only for very short granular

samples. Quantitative limits for this phenomenon inside the granular media deserve further investigation (Britan et al., 1997a).

There are some special features which are unique to the stress measurements inside a bulk of rigid granules. Since the stress is force per unit area, the question, which usually arises, is: how large should the diameter of the transducer be compared with the particle's diameter in order for the stress definition to approximate that of a continuum? While, for most foams this problem is not so important, for granular media it strongly affects the repeatability of the measured results (Britan et al., 1995). In practice, the stress measured at the boundary of the sample can be considered reasonably homogeneous within the entire volume, if the diameter of the transducer is at least 10 times larger than that of the particles (Biarez and Hicher, 1994). For most types of Kistler general-purpose miniature pressure transducers this requirement is met when the particle diameter is $d_p \leqslant 1$ mm. In addition, the diameter and the stiffness of the transducer's sensitive membrane must be as small as possible in order to exclude effects related to the presence of the transducer inside the layer. Owing to the severity of these two problems only wall-flush mounted transducers and granular materials of small particles were used in the present study.

Another point to note is that related to the adequacy of the side-wall measurements and the repeatability of the results obtained for the granular media. The small tube size leads to some concern regarding the one-dimensional behavior of the stress field due to possible arching effect. Moreover, such measurements, in principle, do not reflect the internal conditions well enough because the axial stress which is applied by the shock wave gives rise first to a proportional side-wall frictional drag, and reaches the transducer only after it is transmitted throughout the interior due to the interlocking between the particles. Thus repeatability of such measurements is largely governed by the homogeneity of the granular medium and even small fluctuations in the initial packing can result in different duration total stress profiles and amplitudes (see e.g., Stanly-Wood, 1987). This is an important reason why the repeatability of the data obtained in different tests with similar granular layers is rather poor (Britan et al., 1995).

In the hope of understanding the role of gas filtration on the stress formation, we embarked on a comparative analysis of the compressive stress signals as obtained in experiments with and without gas filtration. Similarly to our previous experiments (see Ben-Dor et al., 1997), the gas filtration was excluded totally by introducing a thin plastic film which plugged the front edge of the granular sample. Since the plastic film was wrapped around the test section corners this method of sealing prevented any leakage and gas penetration into the granular sample at its front edge. Since the method of the sample preparation, which was used in the present study, is still not good enough for obtaining granular media with repeatable characteristics, only compressive stress signals, which were reproduced in several subsequent tests, were used as the basis for comparison purposes. In parallel with this routine several experiments which were aimed at checking another method of homogenizing the granular sample were conducted. In these experiments the granular material was not removed and re-filled after each experiment. Instead, the same material was repeatedly loaded by similar shock waves. It was found that after several repetitions similar stress profiles were obtained.

Typical results of a series of five repeated experiments with a standard granular layer, 64 mm long, are presented in Fig. 5. The pressure traces recorded by transducer G, show the first pressure jump due to the passage of the incident shock wave, and then, the second jump, P_5, behind the shock wave reflected at the granular layer interface. The repeatability of the impact conditions at the entrance is clearly evident. However, at the same time transducers T6 and T8 demonstrate remarkable differences in the amplitude and the profile of the initial unsteady part of the signals which are registered in repeated experiments. While the sharpness of the leading front of these signals in the first and subsequent tests is nearly the same, the length of a small rising precursor in the first test is maximal. Close inspection of the first signal rise clearly shows that the time intervals between this moment in the traces registered by transducers G, T6 and T8 decrease with the test number. Hence, the velocities of the precursors in the second and subsequent tests are larger than in the first one. A simple physical explanation to this fact is as follows. The series of subsequent shock waves compacts the loose parts of the granular medium and the void fraction of the granular sample decrease. As a result, the granular layer becomes stiffer, its damping characteristics decrease and the waves, after several shock waves, travel faster. Note that Yanagisawa (1983) observed similar features for the steady loading of the granular sample in subsequent tests.

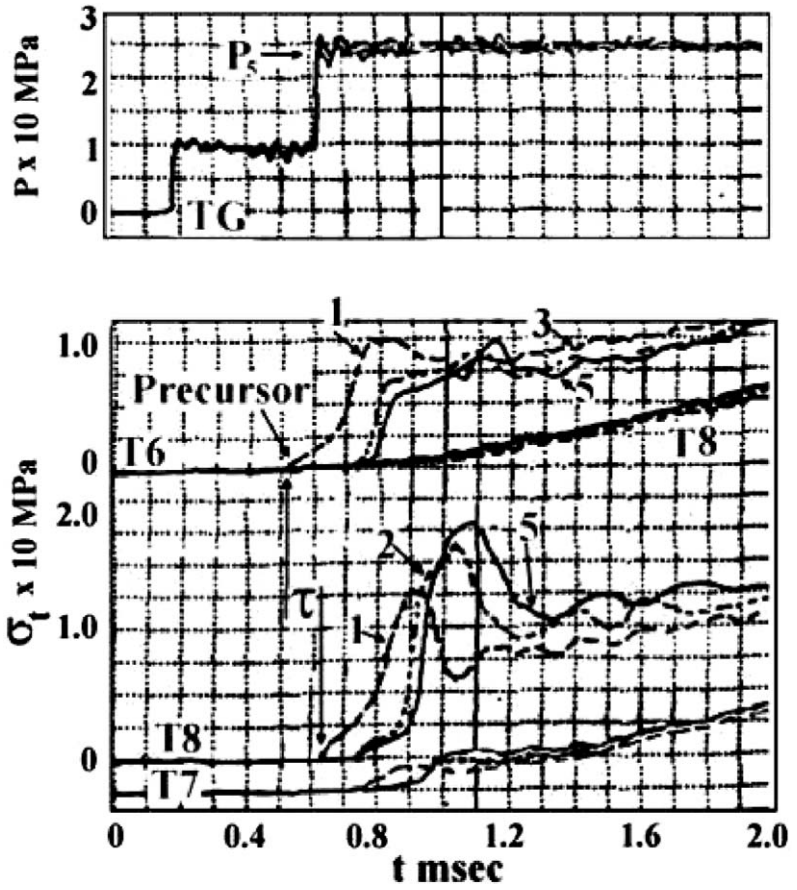

Fig. 5. Initial unsteady part of the compressive stress and the gas pressure signals as obtained in five subsequent tests with the standard granular layer. The numbers on the curves refer to the serial number of the test. Signals 3 and 4 (not shown) lie too close to each other and fall between signals 2 and 4. Material N1 of Table 1, sample thickness $h = 64$ mm. Zero offset for the signal T7 has been used for the sake of convenience purposes only.

We now consider the experimental results shown in Fig. 6. Similar to the previous case the signals registered by pressure transducer G demonstrate good repeatability of the impact conditions. Moreover, unexpected common analogy to the above-mentioned effects is also observed for the unsteady part of the total stress curves. From comparative analysis of the signals shown in Fig. 6 it appears that the main difference in the total stress signals takes place between the results of the first and the second experiment and for subsequent tests it becomes minimal. Thus, similarly to the previous case, subsequent impacts of the protected granular sample in series of two or three equal velocity shock waves is a proper method to homogenize the granular medium and increase its stiffness.

Another important conclusion, which follows immediately from the comparison of the data shown in Figs. 5 and 6, regards the effect of the gas filtration on the peak values of the total stress signals. In fact, while for a standard layer the pressure amplification factor is about $\delta_m = 0.7$, for a protected one it reaches only $\delta_m = 0.24$ (compare these data with those shown in Figs. 1–3 for the polyurethane foams and rubber). Thus, the gas filtration increases the peak of the amplitude of the total stress signals.

A comment is needed regarding the reason for the origin of the precursor in the stress signals. In a previous paper we referred to it as a gas surge which moves ahead of the compaction wave front (Britan et al., 1997a). However, after a closer look at the data in Fig. 5, such a filtration concept seems to be a misleading since owing to the small permeability of this material, the gas pressure starts to rise long after the formation of the precursor; namely, once the compaction wave front reached the transducer. It seems reasonable to

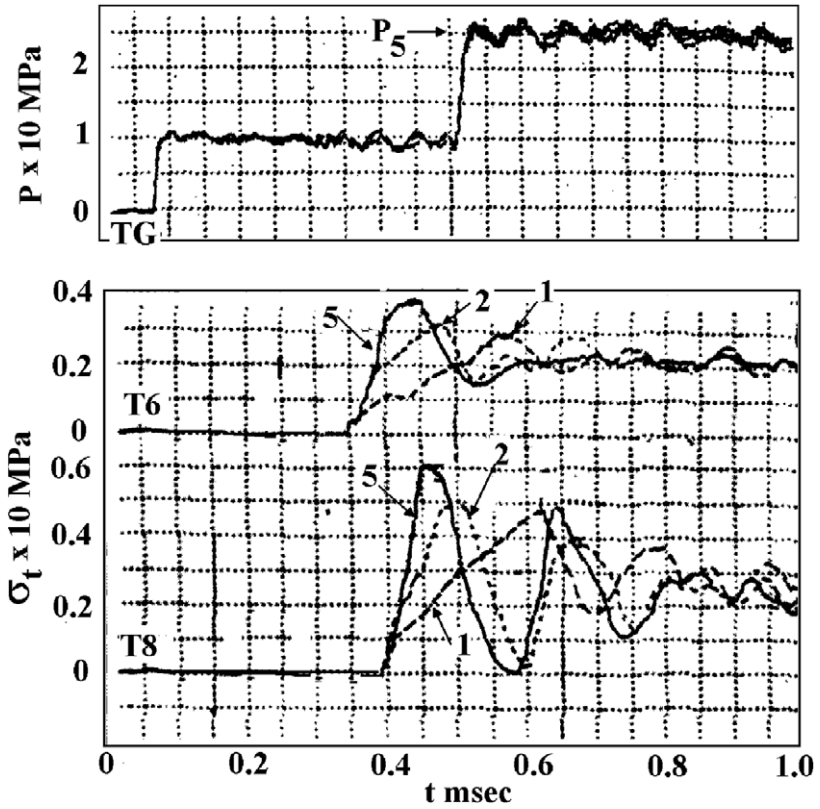

Fig. 6. Initial, unsteady part of the compressive stress signals obtained in five subsequent tests with a protected granular layer. Material N1 of Table 1, and thickness $h = 64$ mm. The numbers on the curves refer to the serial number of the test. Signals 3 and 4 (not shown) lie too close to each other and fall between signals 2 and 5.

suppose, following Skews et al. (1993), that the gas which initially filled the void between the particles was pushed forward by the compaction wave towards the uncompressed granular medium and caused an initial increase in the stress curves. On the other hand, a precursor was not observed in the stress signals of Fig. 6 when the filtration was excluded, thus, correlation of this phenomenon with filtration effect is likely to be through the amplitude of the stress at the front of the compaction wave. The stronger compression that is caused by the stronger compaction wave results in a larger pressure gradient inside the pores and thus the precursor becomes stronger. Since inside the standard (not protected) sample the compaction wave is strong, a precursor appeared here. For a protected sample the compaction wave is about five times weaker than that of a standard one, and hence a precursor was not formed in the case shown in Fig. 6.

To illustrate the role of gas filtration in the formation of the stress in the post-peak period, the signals of Figs. 5 and 6 were reproduced in a longer time scale in Figs. 7 and 8. The repeatability of the gas conditions ahead of the granular layer is quite pronounced. A steady level of the gas pressure, P_5, is terminated by the strong pressure reduction due to arrival of the rarefaction wave, which was reflected from the end-wall of the driver. The maximal discrepancy between the results of subsequent tests during the post-peak period in Fig. 7 does not exceed $\Delta\sigma_t = \pm 9\%$ and does not show any dependency on the test number. However, at first glance it seems strange that these signals remain constant when the rarefaction waves, which are reflected from the end-wall of the driver, reduce the gas pressure ahead the layer by about one-half. This behavior clearly points on the well known "Cotter effect" or arching between the particles which with no gas filtration preserves the magnitude of the total stress inside the sample (Britan et al., 1997a).

The signals in Fig. 8 demonstrate some phenomena, which are unique to the experiments with a standard unprotected sample. The first phenomenon is that the total stress progressively increases due to the increase in the gas pressure, P, in course of the gas filtration. Therewith the increasing rate is not sensitive to a great extent

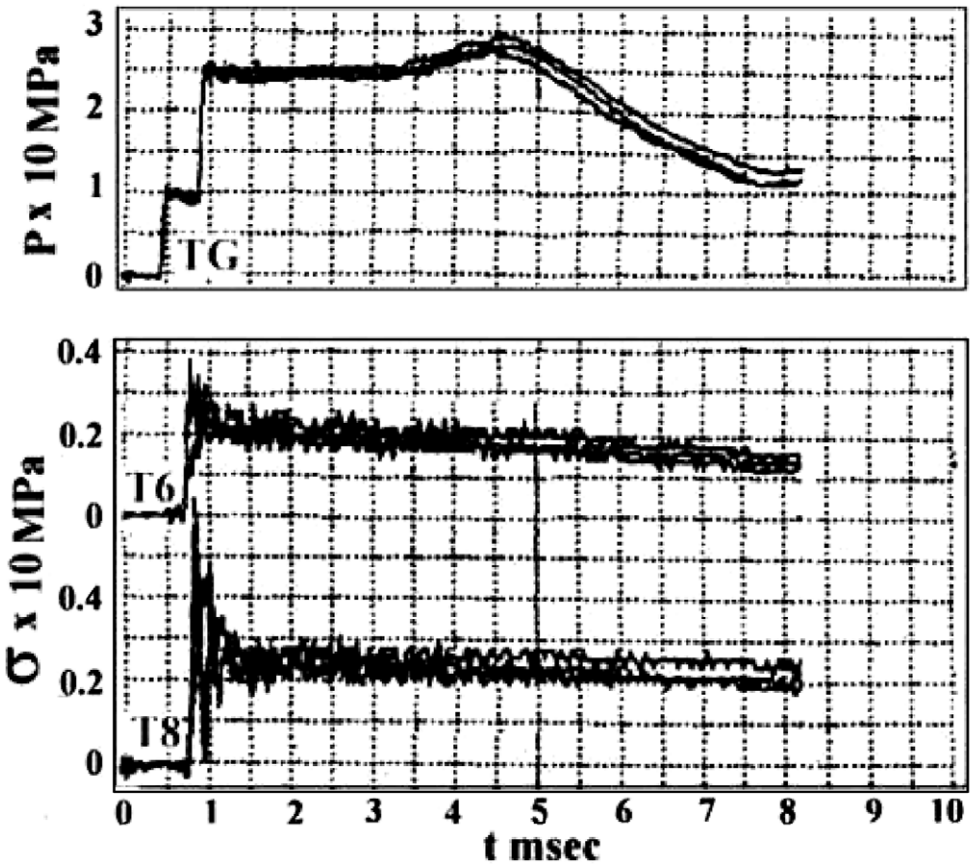

Fig. 7. Typical compressive stress signals obtained in five subsequent tests with the protected granular layer. Material N1 of Table 1, and thickness $h = 64$ mm (full scale presentation).

to the subsequent shock wave loading (the maximal discrepancy between the amplitudes in the first and in the subsequent tests does not exceed about $\Delta\sigma_t = \pm 12\%$).

The second phenomenon is a weak unsteady spike in the gas pressure signals registered by transducer T7 which is closely related to the piston effect, or in other words, to the compaction wave arrival at the end-wall (compare with the signals in Fig. 2a that were obtained with the foam slab F2).

Thirdly, note that in contrast to the data in Fig. 7 the total stress and the gas pressure quickly decrease once the rarefaction wave arrives at the sample interface. This is a clear evidence of the fact that the gas filtration is a very efficient tool in the stress – relieve inside the sample when it is subjected to a weak shock wave impact.

4.2. Effective stress as a dynamic characteristic of unsteady flow pattern

Once the incident shock wave impacts the granular medium the stress conditions inside the bulk are related to the variations in the pressure rise:

$$\Delta P = P_5 - P_g,$$

where P_5 is the gas pressure behind the shock wave that is reflected at the granular layer interface, and P_g is the local gas pressure acting in a cross-section of the granular medium. The pressure rise ΔP is transmitted throughout the interior and due to local variations in the sample porosity π it affects the total stress which is usually registered in the experiments by the pressure transducers. Even though the total stress history which is similar to the curves shown in Fig. 8 carries information on the sample compression and recovering, it is not entirely suitable for reconstructing the unsteady flow pattern inside the granular sample. Gas filtration and

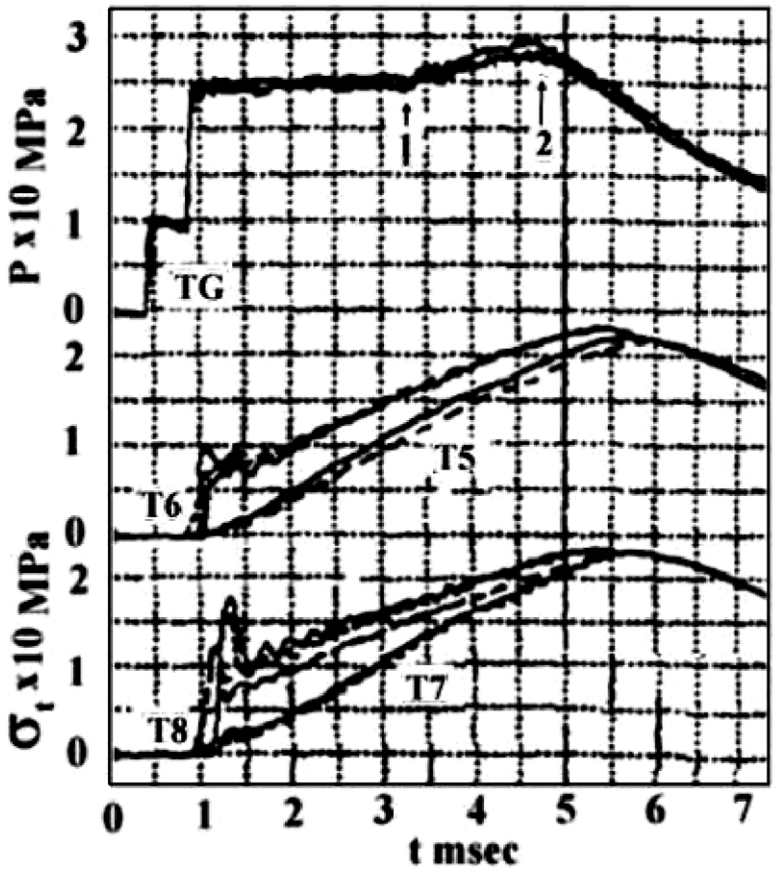

Fig. 8. Typical compressive stress and gas pressure signals obtained in five subsequent tests with the standard granular layer. Material N1 of Table 1, and thickness $h = 64$ mm (full scale presentation).

dissipation effects tend to smooth out sharp variations and marked points in the stress profile which may help to specify the unsteady waves propagation near the transducer. An additional reason which make such an analysis rather complicated, is that all the variations in the bulk volume during a weak shock wave impact are too small to be observed. Thus they deserve further information which is more sensitive to this phenomenon.

All these arguments led us to the assumption that the magnitude of the effective stress or the stress between the particles, $\sigma = \sigma_t - P_g$ would be more suitable for this purpose since it is precisely the parameter responsible for the deformation and strength of the granular medium (see e.g., Lade and De Boer, 1997). In the experiments with unprotected samples the effective stress σ propagates inside the bulk by the gas filtration and directly through the contact points between the particles from the granular layer interface to the measured cross-section. While each of these two processes manifests itself in different ways depending on the sample length, h and its permeability, f (Britan et al., 1997a), in the following the effective stress curves obtained with small and large permeability granular layers of different lengths are presented and compared to each other.

4.3. Small permeability granular layers ($f = 0.00027$ mm^2)

The effective stress profiles, without and with gas filtration, as obtained for a granular layer of material N1 of Table 1 having a small permeability of $f = 0.00027$ mm^2 are shown in Figs. 9 and 10, respectively. The stress curves in Fig. 10 present a computerized subtraction of the gas pressure P_g from the end-wall total stress σ_t, and thus similar to the data in Fig. 9 it comprises the effective stress. One distinctive property of these stress

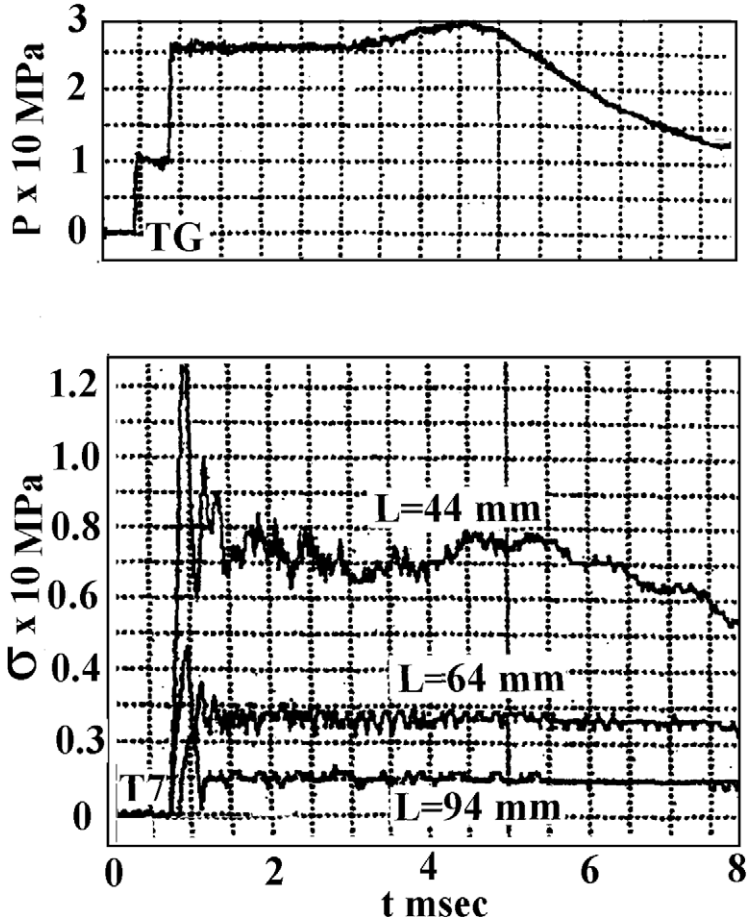

Fig. 9. Typical effective stress signals obtained in five subsequent tests with the protected granular layer of material N1 of Table 1.

profile curves is that, in Fig. 10 when gas filtration took place, it provided in fact an additional compressive force (a drag force) that acted on the particles. Several comments are needed regarding these effective stress histories.

Since the effective stress in Fig. 9 is smaller than that in Fig. 10 one can readily conclude that the drag force strongly affects the effective stress values. Furthermore, comparing the values of the effective stress with those registered by transducer G indicates that the effective stress is much smaller than the gas pressure behind the shock wave which was reflected at the granular layer interface, and that it decreases towards the sample rear-end. All these facts are clear evidences of the energy loss in course of the filtration process.

The next comment concerns with the initial unsteady peak in the stress curves. While it resembles a typical pressure jump across the pressure wave propagating inside the granular medium, the peaks of the amplitudes and the profile are most likely results of several complicated features interacting with each other. The most important of these is an elastic bulk resistance to the compression (inside the volume and near the walls). Since the peaks of the amplitudes in Figs. 9 and 10 are similar regardless the fact whether or not gas filtration took place, dry friction, rotation and sliding of the particles during the change in its packing structure are the leading mechanisms in the formation of the peaks in the stress (Britan et al., 1997a). The second important feature is an effect of unsteady wave interactions inside the granular medium. The amplitudes of the curves in the post-peak period are steady during the full test time in Fig. 9 while in Fig. 10 it is seen to start to decrease dramatically after some time. If one supposes that the decrease is caused by the rarefaction wave which originates inside the sample after the reflected wave interacts with the sample interface (see e.g., Skews et al., 1993), the time elapse between the first increase in the signal and the onset of the decrease must be coincident with

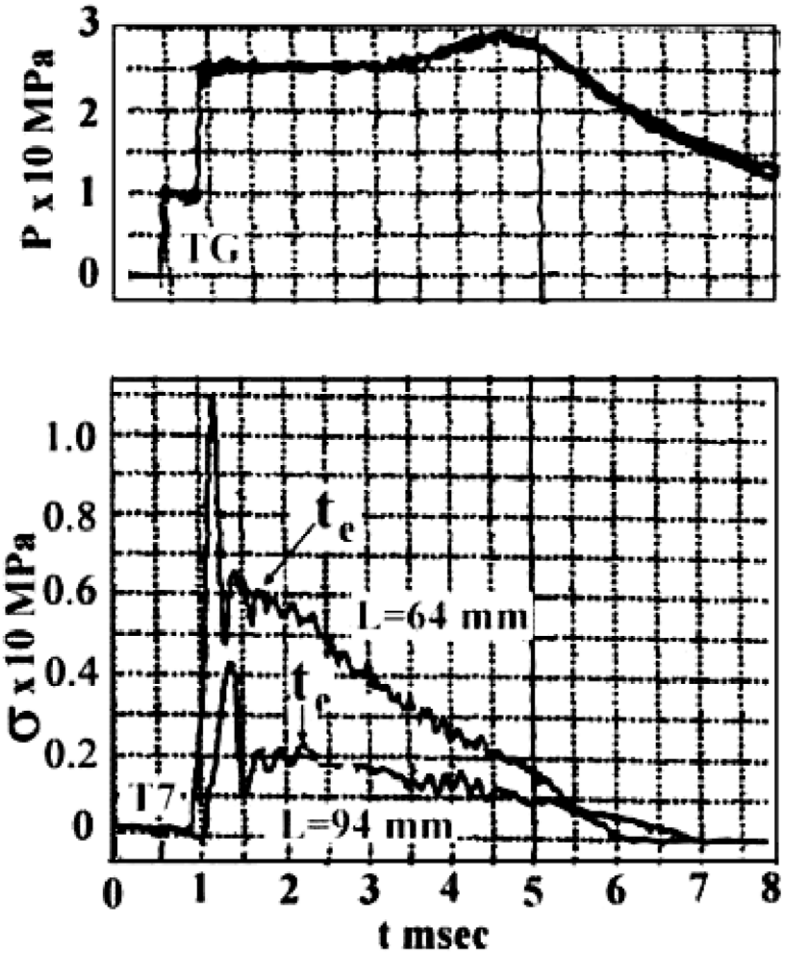

Fig. 10. Typical effective stress signals obtained with the standard granular layer of material N1 of Table 1.

the test-time period for the end-wall measurements. Clearly, during this test time the end-wall conditions are independent on any variation in the flow parameters at the granular layer interface.

Assuming that the velocities of the transmitted (V_g) and compaction (V_s) waves remain constant in course of their reflection at the end-wall, the end-wall test time can be estimated from

$$t_e = \frac{h(3V_s - V_g)}{V_g V_s}. \tag{1}$$

The values of t_e shown by arrows in Fig. 10 were obtained using Eq. (1) and the experimental data for V_s and V_g as reported by Ben-Dor et al. (1997). The fact that these values agree quite well with the onset of the signal decrease lends further support to the validity of Eq. (1) for estimating the end-wall test time.

Since most of the processes involved in the particle–particle interaction are frictional in their nature, they must be sensitive to the variation in the granular layer length h. In agreement with this statement the peaks of the amplitude in the cases shown in Figs. 9 and 10 indeed decrease in the course of the compaction wave propagation along the sample.

The particle diameter, d_p, is another factor affecting the effective stress formation. Since the granular layer permeability increase with d_p, this must be accomplished by an increase in the transmitted wave velocity V_g and other effects related to the compaction wave formation (Ben-Dor et al., 1997). On the other hand, increasing V_g decreases t_e and the rarefaction wave reaches the end-wall before the gas–solid interaction has been completed. Thus, inside granular materials of large particles the impact energy will not be transmitted completely to the end-wall during the test time and as a result the effective stress would be smaller.

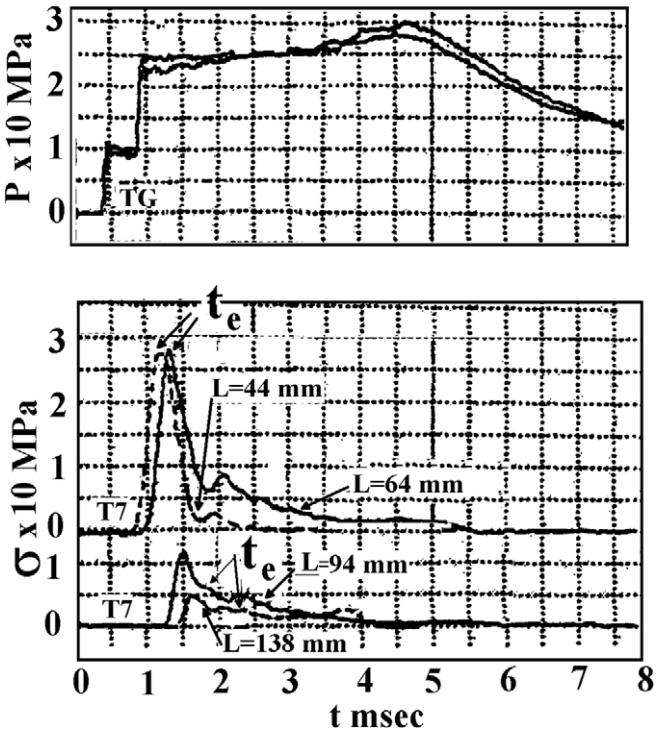

Fig. 11. Typical effective stress signals obtained with the standard granular layer of material N2 of Table 1.

4.4. Large permeability granular layers (0.00099 mm^2)

To illustrate this phenomenon the effective stress profiles as obtained with the standard samples of material N2 of Table 1 are shown in Fig. 11. Comparative analysis of these signals revealed many features common with those in Figs. 9 and 10. In addition the following should be mentioned.

As can be seen in Fig. 11, inside the granular samples having lengths of $h = 44$ mm and $h = 64$ mm the gas filtration actually causes a strong rarefaction wave, which limits the amplitude of the unsteady effective stress peak and affects the post-effective stress peak profile of the σ curves. This feature prevents correct comparison of such profiles with the quasi-steady profiles that were obtained when the gas filtration was blocked.

For the longest granular samples the rarefaction wave reaches the end-wall after the unsteady peak formation. In addition, the peak in the σ curves that was obtained with the sample of length $h = 94$ mm when gas filtration took place is nearly twice larger than that when the gas filtration was blocked. There is no doubt that filtration must be accomplished by strong energy losses and thus it attenuates with distance along the granular sample. As its contribution to the transition of the stress through the contact points of the particles would also attenuate with the sample length, h, so does the effective stress. Consequently, maximal compression would be observed close to the sample interface and will decreases towards its rear-end.

5. Discussion

From the results shown in Figs. 9–11 it is evident that large particles are more productive in the formation of a peak stress than small ones. In practice, this trend is valid only for the profiles illustrated in these figures and beyond this range it can be reversed. To ensure this, the peak stress data, P_{max}, as measured within a wide range of operating conditions are presented in Figs. 12–14 for the cases in which gas filtration takes and does not take place. It is clearly seen from these figures that

(a) In similar to foams, for each type of granular medium there is an "optimal" layer length, h^*, which results in a maximum in the curve $P_{max} = P(h)$.
(b) The optimal granular layer length, h^*, depends on the diameter, d_p, and the particle density ρ_p. In fact, the maximal peak stress for two materials N1 and N3 that consist of particles of similar diameter, d_p, occur at different values of h^*.
(c) For all the data obtained with samples in which the gas filtration was blocked, the values of P_{max} are smaller than those for samples when gas filtration took place. Thus the gas filtration has a non-negligible effect on the total stress formation.

The data in Figs. 12–14 are very important in constructing the dynamic relation between the average normal stress σ_a and the sample deformation ε (see e.g., Lakhov and Polyakova, 1972). Since the granular medium fills all entire cross-section of the channel the particles can move only along the test section axis x. Hence, during the shock wave impact a uni-axial compression takes place and the sample compression ε_1 is along the direction of propagation of the impacting shock wave. Therefore

$$\varepsilon_2 = \varepsilon_3 = 0, \tag{2}$$

$$\sigma_2 = \sigma_3 \neq 0, \tag{3}$$

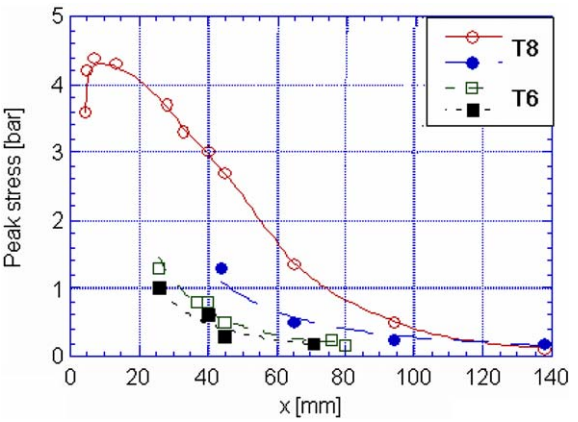

Fig. 12. The dependence of the maximum value of the total stress on the length of the sample. The experimental data were obtained with a standard sample (open symbols) and with a film-protected sample (closed symbols) of material N1 of Table 1.

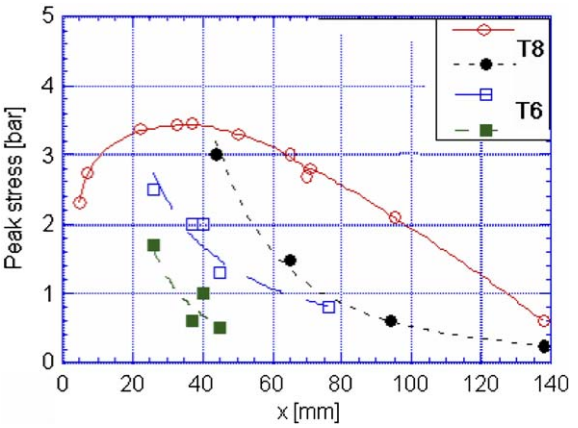

Fig. 13. The dependence of the maximum value of the total stress on the length of the sample. The experimental data were obtained with a standard sample (open symbols) and with a film-protected sample (closed symbols) of material N2 of Table 1.

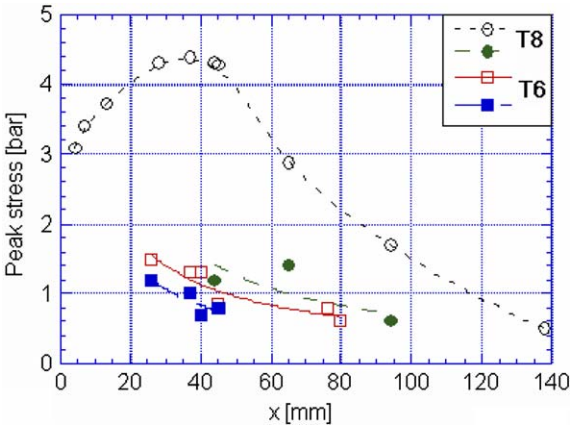

Fig. 14. The dependence of the maximum value of the total stress on the length of the sample. The experimental data were obtained with a standard sample (open symbols) and with a film-protected sample (closed symbols) of material N3 of Table 1.

where ε_2, ε_3 and σ_2, σ_3 are the lateral (tangential) deformations and stresses, respectively. The principal stresses σ_1, σ_2, σ_3 are related to the average normal stress σ_a through

$$\sigma_a = -\frac{1}{3}(\sigma_1 + \sigma_2 + \sigma_3). \tag{4}$$

In the case of motions with plane symmetry in view of Eq. (3), we have

$$\sigma_a = -\frac{1}{3}(\sigma_1 + 2\sigma_2). \tag{5}$$

If the sample deformation ε is related to the density ρ through

$$\varepsilon = \frac{\rho_c - \rho}{\rho}, \tag{6}$$

where ρ_c is the initial bulk density of the granular medium, the laws of conservation of mass and linear momentum at the shock wave front, enable us to obtain the following simple equation defining the dynamic compression of the granular medium at the shock wave front:

$$\varepsilon = -\frac{3\sigma}{(1+2k_\tau)\rho_0 V_g^2}, \tag{7}$$

where $k_\tau = \sigma_2/\sigma_1$ is the coefficient of lateral stress.

Eq. (7) is valid only if the transmitted pressure wave is a shock wave. Note that in the experiments the peak of the stress profile depends on the pressure transducer, on its way of installation inside the test section, on the type of the granular medium and on the intensity of the impacting shock wave. Moreover, even if all the theoretical requirements for the transformation of the compression wave to a shock wave inside the bulk are met (see e.g., Mazor et al., 1994), it is still not clear how sharp a registered peak must be in order for it to be classified as the stress at the shock wave front. Defining the lowest limits for the validity of Eq. (7) in our conditions is not a simple task. We have tried to use it in our analysis by taking in mind that the tested granular materials do not vary significantly in their characteristics and are compared within the similar range of the maximal total stress. When the magnitudes of the bulk density, ρ_c, and the velocity, V_g, are known, the peak stress values registered at the side and at the end-wall can be used as approximations for σ_1 and σ_2. Thus, the data shown in Figs. 12–14 are attractive for obtaining the relation between k_τ and σ_a for a granular layer of length h. Furthermore, if the length, h, is excluded, the dynamic equation (7), allows one to define the granular layer deformation, ε, as a function of the average normal stress, σ_a, at the shock wave front. The obtained results are compared in Fig. 15 with curve N4 which was obtained by Lakhov and Polyakova (1972) during

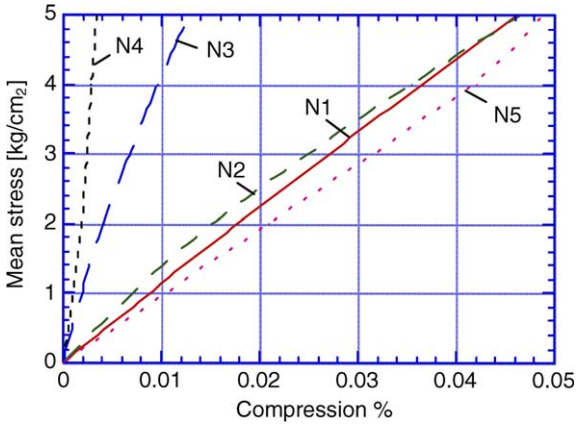

Fig. 15. Stress–strain curves for the granular materials under study. The numbers of the curves refer to the material code number of the granular medium as defined in Table 2.

field tests with explosive waves and with curve N5 which is a result of the shock tube experiments of Lakhov (1968). The data in Fig. 15 as well as the main characteristics of the granular materials under discussion (shown in Table 2) offer a clear view of compression phenomenon and its relation to the type of the granular medium.

It is clearly seen from these data that depending upon the material characteristics similar stress results compressions, which may differ by more than a factor of 10. While all granular media have nearly the same porosity $\pi \approx 0.4$, the air content in the clayey soil (material N4) is mostly replaced by water and thus the compression of the clayey soil is marginal. According to the data in Table 2 it must behave as an ideal liquid with almost similar normal and lateral stresses ($k_\tau = 0.9$) and for the studied conditions material N4 has maximal Young's module $E_d = 1000\ \mathrm{kg/cm^2}$. Taking this value of E_d as indicative of the limiting value of the dynamical Young's module, the next in stiffness is a sample of material N3 with a Young's module $E_d = 375\ \mathrm{kg/cm^2}$. A lesser value of the coefficient k_τ shows that its behavior must be closer to the solid medium whose stiffness is dictated by the skeleton density $\gamma = \rho_s\rho_c/\rho_p$. When γ is large, the granular medium is densely packed and thus, a stronger force is required to compress it (Lakhov and Polyakova, 1972). The next parameter responsible for the granular sample compression is the ratio of the mean area of the particles contacts to the mass of the particle. A granular medium of spherical particles, which are arranged in a uniform array, has limited number of contacts per particle, corresponding to the material porosity. Let us consider materials N2 and N3, which have similar porosities and skeleton densities γ, but different particle diameters (material N2 consists of larger particles). Since the mass of the particle increases with d_p the tenacity of material N2 is smaller and it could be compressed more easily. On the other hand, the dynamic Young's module for material N2 is about $E_d = 129\ \mathrm{kg/cm^2}$, which is close enough to that of materials N1 and N5 ($E_d = 110\ \mathrm{kg/cm^2}$ and $E_d = 95\ \mathrm{kg/cm^2}$, respectively) having similar skeleton density $\sigma_t = \sigma_{t\,max}$.

Table 2
The main characteristics of the granular materials

N	Material	π	k_τ	V_g, m/s	V_s, m/s	γ	Water content, %
1	Potash	0.428	0.2-0.4	144	236	1.17	–
2	Fe 1.04 mm	0.393	0.2	226	170	4.50	–
3	Fe 0.45 mm	0.399	0.6	143	175	4.46	–
4	Clayey soil	0.011	0.9	–	–	2.01	12-15
5	Sand	0.432	0.3-0.4	80	–	1.50	–

π – initial porosity, k_τ – coefficient of lateral stress, V_g – transmitted wave velocity, V_s – compaction wave velocity, γ – skeleton density.

6. Summary and conclusion

The compression phenomenon during the impact of weak shock waves on granular layers of different characteristics has been addressed. A variety of the gas flow–skeleton interactions and the compression history of the samples were studied under similar loading conditions.

1. The role of the filtration and unsteady phenomena inside the sample were analyzed. They suggested the followings:
   (a) The shock-induced gas filtration is responsible for the total stress formation at the end-wall and may increase it peak values up to four times due to the drag force acting on the granules. Since the filtration effect is accomplished by energy losses its contribution to the particle–particle interaction attenuates with distance along the sample and so does the effective stress.
   (b) Based on a simple refraction model of the unsteady wave propagation it was shown that the rarefaction reflected back into the sample as a result of the transmitted wave refraction at the sample interface, similar to the case of flexible foams, may restrict the peak of the amplitude of the total stress signal inside the granular medium. As in the case of any filtration process, the role of such an effect on the stress formation increases with the permeability of the granular medium and decreases towards the sample rear-end.
   (c) For each kind of granular medium there is an optimal layer length exist, h^*, which results a peak value of the total stress. Beyond this length two different phenomena are of importance for the peak stress formation: for short layers, when $h < h^*$ the peak stress amplitude can be restricted by the rarefaction wave arrival; while for long layers of $h > h^*$ the peak profile of the total stress is mostly governed by the elastic bulk resistance to the compression in course of the particle–particle interaction.
   (d) The strong effect of the gas filtration demonstrates also the rarefaction wave reflected from the end-wall of the shock tube driver (see e.g., the signals in Fig. 8). Reaching the sample interface this expansion wave catches up with the high pressure region inside the totally compressed sample and the gas which is flowing out acts as a very efficient tool in the stress release. Notably, whereas the rarefaction wave reaches the thin film which blocks the gas filtration, the pressure reduction at the sample entrance can be also transmitted into the granular medium. The data in Fig. 9 clearly show for this case that the stress-release without gas filtration, namely, which results only from particles contacts is less efficient and can be observed only inside the shortest sample.
2. Based on the peak stress measurements at the side-wall and at the end-wall of the test section a dynamic stress–strain relation between the average normal stress and the sample deformation was constructed. Attempts to define such characteristics has been prompted by the need to design protectors against shock wave loading on man-made structures. Comparative analysis of the compression curves clearly shows that depending on the material stiffness, similar stress results the sample compression, which may differ by more than a factor of 10. The stiffness and dynamic Young's module, E_d, for the bulk of small Fe particles (material N3) is the largest among the three types of granular media which were used in this study. In contrast to that, sample of potash (material N1) consisting of light particles of similar diameter demonstrated maximal flexibility and a smallest value of dynamic Young's module ($E_d = 95$ kg/cm^2). Moreover, while a decrease in Young's module results in a smaller sound velocity, one may conclude that in choosing between two such materials, a bulk of material N1 is more suitable for attenuation purposes.
3. An effective method to homogenize the granular media has been proposed. It allows to improve the repeatability of the total stress measurements. According to our observations, after loading of the granular sample by several (two or three) equal velocity shock waves, the amplitude and profile of the total stress signals, which are obtained in subsequent tests with the same sample repeat with an accuracy of about 10%.

There are many ways to extend this work. To the best of our knowledge, much remains to be done theoretically in terms of addressing the above-mentioned issues (1)–(3). In this relation we would like to encourage our colleagues to simulate impact phenomenon of granular medium for the conditions studied in the experiments including the effects of the gaseous phase. Such research would allow to better understand many questions, which have been left open in the course of the present study.

Acknowledgements

We are indebted to Prof. Zaretzky for valuable discussions. The work was partially supported by the Israeli Science Foundation under Grant Nos. 190/01, 278/03, 154/04 and United State Israel Bi-national Science Foundation under Grant No. 2000-0050.

References

Baer, M.R., 1988. Numerical studies of dynamic compaction of inert and energetic granular materials. Appl. Mech. 55, 36–43.

Bazhenova, T.V., Gvozdeva, L.G., Lagutov, Yu.P., Lakhov, V.N., Faresov, Yu.M., Fokeev, V.P., 1986. Unsteady interaction of shock and detonation waves in gases. Nauka, Moscow (in Russian). Also translated to English under the same title. Russian Ed. V.P. Korobeinikov, English Ed. P.A. Urtiev, Hemisphere, New York, NY, USA, 1988, pp. 48–61.

Bear, J., Bachmat, Y., 1990. Introduction to Modeling of Transport Phenomena in Porous Media. Kluwer.

Ben-Dor, G., Mazor, G., Igra, O., Sorek, S., Onodera, H., 1994. Shock wave interaction with cellular materials. Part 2. Open cell foams; experimental and numerical results. Shock Waves 3, 167–179.

Ben-Dor, G., Britan, A., Elperin, T., Igra, O., Jiang, J.P., 1997. Experimental investigation of the interaction between weak shock waves and granular layers. Exp. Fluids 22, 432–447.

Biarez, J., Hicher, P.Y., 1994. Elementary Mechanics of Soil Behavior. Balkema, Rotterdam, Holland.

Blazynsky, T.Z., 1987. Explosive compaction of nonmetallic powder mixtures. In: Briscoe, B.J., Adams, M.J. (Eds.), Tribology in Particulate Technology. Adam Higer, Bristol, England, pp. 303–315.

Britan, A., Elperin, T., Igra, O., Jiang, J.P., 1995. Head-on collision of a planar shock wave with a granular layer. In: Schmidt, S.C., Tao, W.C. (Eds.), Proceedings International Shock Compression of Condensed Matter Conference, Part 2. The American Physical Society, Seattle, WA, USA, pp. 971–974.

Britan, A., Ben-Dor, G., Elperin, T., Igra, O., Jiang, J.P., 1997a. Mechanism of compressive stress formation during weak shock waves impact with granular materials. Exp. Fluids 22, 507–518.

Britan, A., Ben-Dor, G., Elperin, T., Igra, O., Jiang, J.P., 1997b. Gas filtration during the impact of weak shock waves on granular layers. Int. J. Multiphase Flow 23, 473–491.

Dullien, F.A., 1992. Porous Media. Academic Press, New York, NY, USA.

Gelfand, B.E., Gubin, S.A., Kogarko, S.M., Popov, O.E., 1975. Investigation of propagation and reflection of pressure waves in porous media. J. Appl. Mech. Tech. Phys. 16, 74–81.

Gelfand, B.E., Gubanov, A.V., Timofeev, E.J., 1983. Interaction of shock waves in air with a porous screen. Izv Akad SSSR Mekh Zhidkostei Gaza 4, 78–84.

Gvozdeva, L.G., Faresov, Yu.M., Fokeev, V.P., 1985. Interaction between air shock waves and porous compressible materials. J. Appl. Mech. Tech. Phys. 26, 111–115.

Gvozdeva, L.G., Faresov, Yu.M., Sharov, Yu.L., 1993. Structure of deformation waves in porous compressible materials under the influence of shock waves. Proceedings of 19th International Symposium on Shock Waves, Marseille, France, vol. 3. Springer, Berlin, Germany, pp. 176–180.

Gvozdeva, L.G., Lagutov, Y.P., Sharov, Yu.L., Sherbak, N.B., 1996. Structure of deformation waves in porous compressible materials – influence of percolation. Proceedings of 20th International Symposium on Shock Waves, Pasadena, California, USA, vol. 2. World Scientific, pp. 1393–1400.

Holster, S.R., Brennen, C.E., 2005a. Pressure wave propagation in a granular bed. Phys. Rev. E 72, 031303 1–031303 13.

Holster, S.R., Brennen, C.E., 2005b. Pressure wave propagation in a shaken granular bed. Phys. Rev. E 72, 031303 1–031304 6.

Igra, O., Wang, L., Ben-Do, R.G., Reichenbach, H., Heilig, W., 1997. Uni-axial strain loading of a rubber rod by planar shock waves. Acta Mech. 120, 91–107.

Lade, P.V., De Boer, R., 1997. The concept of effective stress for soil, concrete and rock. Geotechnique 47, 61–78.

Lakhov, G.M., 1968. Verification of the soil viscosity. J. Appl. Mech. Tech. Phys., 68–71.

Lakhov, G.M., Polyakova, N.I., 1972. Waves in solid media and loads on structures. Foreign Tech. Division Air Force System Command, US Air Force, Wright-Patterson AFB, Ohio, USA.

Mazor, G., Ben-Dor, G., Igra, O., Sorek, S., 1994. Shock wave interaction with cellular materials. Part 1. Analytical investigation and governing equations. Shock Waves 3, 159–165.

Nesterenko, V.F., 2001. Dynamics of Heterogeneous Materials. Springer-Verlag, New York, NY, USA.

Raevsky, D.K., Gvozdeva, L.G., Faresov, Y.M., Bressard, J., Bailly, P., 1990. Reflection of shock and explosion waves from surfaces covered with layers of polyurethane foam. Presented in 11th International Colloquium Dynamics of Explosions and Reactive Systems, AIAA, p. 171.

Seitz, M.W., Skews, B.W., 1996. Shock impact on porous plugs with a fixed gap between the plug and a wall. Proceedings 20th International Symposium Shock Waves, Pasadena, California, USA, vol. 2. World Scientific, pp. 1381–1386.

Sen, S., Mohan, T.R.K., Visco Jr., D.P., Swaminathan, S., Sokolow, A., Avalos, E., Nakagawa, M., 2005. Using mechanical energy as a probe for the detection and imaging of shallow buried inclusions in dry granular beds. Int. J. Modern Phys. B 1918, 2951–2974.

Skews, B.W., 1991. The reflected pressure field in the interaction of weak shock waves with a compressible foam. Shock Waves 1, 205–211.

Skews, B.W., Atkins, M.D., Seitz, M.W., 1993. The impact of a shock wave on porous compressible foams. J. Fluid Mech. 253, 245–265.

Stanly-Wood, N.G., 1987. Uni-axial powder compaction. In: Briscoe, B.J., Adams, M.J. (Eds.), Tribology in Particulate Technology. Adam Higer, Bristol, England, pp. 249–271.

van Dongen, M.E.H., Smeulders, D.M.J., Kitamura, T., Takayama, K., 1995. On wave phenomena in permeable foam. Acustica 81, 63–70.

Yanagisawa, E., 1983. Influence of void ratio and stress condition on the dynamic shear modulus of granular media. In: Shahinpoor, M. (Ed.), Advances in the mechanics and the flow of granular materials, vol. 2. Trans Technical Publications, USA, pp. 946–960.

Yasuhara, M., Kitagawa, K., Sakashita, S., Tsuzaki, Y., Watanabe, S., 1995. One-dimensional shock wave interaction with rubber and low-porosity foam. Shock Waves 5, 25–32.

Yasuhara, M., Watanabe, S., Kitagawa, K., Yasue, T., Mizutani, M., 1996. Experiment on effect of porosity in the interaction of shock wave and foam. Japanese Soc. Mech. Eng.—Int. J., Ser. B 39, 287–293.